INTERNATIONAL JOURNAL FOR NUMERICAL AND ANALYTICAL METHODS IN GEOMECHANICS, VOL. 22, 393–416 (1998)

STRESS–STRAIN MODEL FOR CLAYS WITH ANISOTROPIC VOID RATIO DISTRIBUTION

EYAD MASAD,[1†] BALASINGAM MUHUNTHAN[2‡] AND JEAN LOU CHAMEAU[3§]

[1]*Civil and Environmental Engineering, Washington State University, Pullman, WA 99164, U.S.A.*
[2]*Civil and Environmental Engineering, Washington State University, Pullman, WA 99164, U.S.A.*
[3]*School of Engineering, Georgia Institute of Technology, Atlanta, GA 30332, U.S.A.*

SUMMARY

The porosity of soils is considered to be a directional measure and its distribution is characterized by a functional form. This form has been used to extend the critical state soil mechanics framework to include the effects of structure in soils. A new internal plastic energy dissipation formulation has been proposed to account for fabric arrangement. New expressions for the yield locus, and the plastic stress–strain response of structural soils have been derived. The applicability of the concepts to model the plastic stress–strain behaviour of a number of soils is illustrated. The advantage of the new model is very well identified in modelling the stress–strain behaviour of K_0 consolidated and natural clays. © 1998 John Wiley & Sons, Ltd.

Int. J. Numer. Anal. Meth. Geomech., vol. 22, 393–416 (1998)

Key words: fabric; porosity; tensor; yield; stress; strain

INTRODUCTION

The critical state soil mechanics framework, formulated by the Cambridge school, has provided a coherent foundation for unifying the volumetric and shear behaviour of soils. It has also provided a logical framework for incorporating theories of plasticity, yield, and flow for the mathematical modeling of soil behaviour. In the current applications of the critical state soil mechanics framework, the soil behaviour is captured in a three-dimensional isotropic void ratio-effective normal and shear stress space.

The critical state concept was developed mainly to explain the behaviour of reconstituted, essentially, isotropic, materials. As further experimental information has been obtained, it has become clear that the effects of inherent and induced anisotropy leads to soil behaviour very different from those predicted by the critical state models. These differences stem from the influence of microstructure and macrostructure of clays. Following Mitchell[1] the term 'structure' is referred to as the combination of fabric (arrangement of particles) and interparticle bonding.

[1]Correspondence to: B. Muhunthan, Associate Professor, Civil and Environmental Engineering, Washington State University, Pullman, WA 99164, U.S.A.
[†]Graduate Student.
[‡]Associate Professor.
[§]Dean.

CCC 0363–9061/98/050393–24$17.50

Received 28 October 1996
Revised 25 August 1997

Leroueil and Vaughan[2] presented a detailed summary documenting the effects of structure in natural clays. It was shown that while the structure can arise from many causes, its effects follow a simple general pattern. The sedimentation compression curves for most, but not all natural clays, plot well above those for reconstituted specimens.[2,3] A consequence of this is that such soils are more sensitive and brittle than reconstituted materials and in most cases strain-soften to failure. The strain-softening behaviour becomes more pronounced as the skeletal nature of structure changes.

In some clays, the structure remains intact at low levels of isotropic consolidation pressure in the laboratory. Therefore, fabric effects are evident in the stress–strain behaviour of these soils. They are, however, not as pronounced as those associated with *in situ* and anisotropically consolidated clays. Observations of linear stress–strain behaviour in the post-yield region of a wide variety of lightly overconsolidated or cemented clays is another manifestation of the effect of structure.[4]

The critical state concept has to be modified to account for anisotropic and structural nature of the clay behaviour. Phenomenological models based on rotational hardening have been proposed and shown satisfactorily to account for the effects of anisotropy.[5,6] Unlike in the case of the family of original critical state soil models, the additional parameters used in the latter models have little or no physical meaning attached to them.

The present study proposes a logical extension of the critical state soil mechanisms framework to include the effect of structure in soils. Attention is focused on the effects of fabric. The porosity of structural soils is considered to be a directional measure and its distribution is characterized by a functional form that can be determined experimentally. The energy dissipation formulation has been modified to incorporate the effects of fabric and has been used to derive new expressions for the yield locus, and the plastic stress–strain response of a soil.

FABRIC MEASURE BASED ON VOID SPACE

The mechanical behaviour of soils is strongly influenced by the packing of the individual particles. Porosity or void ratio is often used to characterize the state of packing. These scalar measures, however, are incapable of characterizing the directional nature of fabric. Measures which can reflect the directional nature of fabric in structural soils are needed.

In order to develop directional measures a Representative Element Volume (REV) is chosen. The REV consists of sufficient number of particles to make the statistical treatment valid.[7,8] It can be generally of any shape such as cubical, spherical, etc. An idealized REV with shaded voids is shown in Figure 1. Using averaging techniques within an REV, the distribution of void ratio can be approximated by a directional function $e(\mathbf{I})$ of the form.[7,9]

$$e(\mathbf{I}) = e_{\mathrm{m}}(1 + \Omega_{ij} l_i l_j) \tag{1}$$

where $e(\mathbf{I})$ is the magnitude of the void ratio vector in the direction of the unit vector $\mathbf{I}$, e_{m} is the isotropic void ratio of the soil, the components of the unit vector $\mathbf{I}$ are given by $l_1 = \sin\theta \sin\phi$, $l_1 = \cos\theta$ and $l_3 = \sin\theta \cos\phi$ (Figure 1), and Ω_{ij} is termed the void fabric tensor. The components of the void fabric tensor represent the deviations from the isotropic distribution of voids. If the voids are isotropically distributed, the components of the void fabric tensor become zero and equation (1) reduces to the average value, e_{m}, of the void ratio. These components can be obtained from microscopic observations within a representative elemental volume (REV). Complete derivation of equation (1) is given by Muhunthan *et al.*[7]

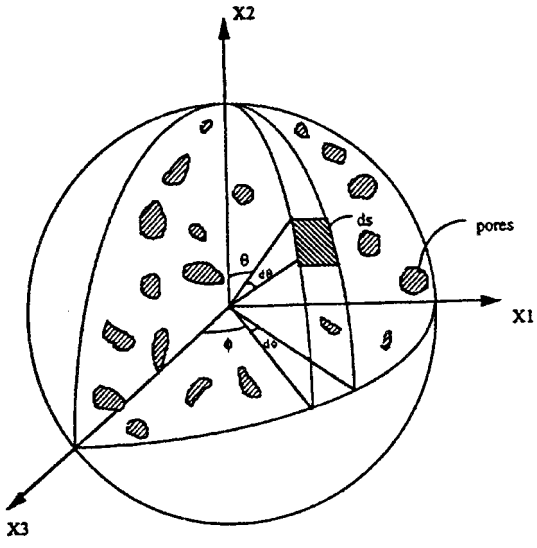

Figure 1. The coordinate system used in the void fabric tensor analysis

The specific volume $v = 1 + e$ has often been used in the development of concise critical state based stress–strain models for soils. The magnitude of the specific volume in **I**-direction, $v(\mathbf{I})$, follows from the directional void ratio as:

$$v(\mathbf{I}) = v_{\mathrm{m}} + \phi v_{\mathrm{m}} - \phi \tag{2}$$

where $\phi = \Omega_{ij} l_i l_j$ and v_{m} is the isotropic specific volume.

FABRIC AND STRAIN

For small strains, the volumetric strain increment, $\mathrm{d}\varepsilon_v$, is equal to the incremental change in volume divided by the current volume. Since the change in volume equals the change in volume of voids, the volumetric strain increment can be expressed by

$$\mathrm{d}\varepsilon_v = \mathrm{d}v/v \tag{3}$$

Substitution of the directional specific volume (equation (2)) in the above expression leads to

$$\mathrm{d}\varepsilon_v = \frac{\mathrm{d}(v_{\mathrm{m}} + \phi v_{\mathrm{m}} - \phi)}{v_{\mathrm{m}} + \phi v_{\mathrm{m}} - \phi} \tag{4}$$

or

$$\mathrm{d}\varepsilon_v = \frac{v_{\mathrm{m}} + \phi v_{\mathrm{m}}}{v_{\mathrm{m}} + \phi v_{\mathrm{m}} - \phi} \left(\frac{\mathrm{d}v_{\mathrm{m}}}{v_{\mathrm{m}}} + \frac{v_{\mathrm{m}} - 1}{v_{\mathrm{m}} + \phi v_{\mathrm{m}}} \mathrm{d}\phi \right) \tag{5}$$

or

$$\mathrm{d}\varepsilon_v = \frac{v_{\mathrm{m}} + \phi v_{\mathrm{m}}}{v_{\mathrm{m}} + \phi v_{\mathrm{m}} - \phi} \left((\mathrm{d}\varepsilon_v)_{\mathrm{m}} + \frac{v_{\mathrm{m}} - 1}{v_{\mathrm{m}} + \phi v_{\mathrm{m}}} \mathrm{d}\phi \right) \tag{6}$$

Note that $(\mathrm{d}\varepsilon_v)_{\mathrm{m}}$ is the average volumetric strain increment measured in a conventional triaxial test and used in isotropic models, while $\mathrm{d}\varepsilon_v$ is the volumetric strain increment that considers the fabric variation in the direction of the unit vector 1.

Since the fabric tensor Ω_{ij} is deviatoric, it is possible to relate its change to the deviatoric or shear strain change, $\mathrm{d}\varepsilon_{ij}$, through the use of an isotropic tensor valued functional representation:

$$\mathrm{d}\Omega_{ij} = \mathrm{d}\Omega_{ij}(\Omega_{kl}, \mathrm{d}\varepsilon_{kl}, v_{\mathrm{m}}) \tag{7}$$

The functional form is generally complex. However, if the principal axes of $\mathrm{d}\varepsilon_{ij}$ and $\mathrm{d}\Omega_{ij}$ are assumed to be coincident, the relation can be modeled as:[7]

$$\mathrm{d}\Omega_{ij} = \beta\, \mathrm{d}\varepsilon_{ij} \tag{8}$$

with

$$\beta = a_1(1 - l/v_{\mathrm{m}}) + a_2(1 - l/v_{\mathrm{m}})\Omega_{ik}\Omega_{ki} \tag{9}$$

where a_1 and a_2 are scalar functions of the isotropic specific volume. The relationship between fabric and the strain deviator tensor has also been studied by Kanatani.[10] Denoting $\mathrm{d}\varepsilon_{ij}l_i l_j = (\mathrm{d}\varepsilon_q)'$, the shear strain increment in l-direction, equation (8) becomes

$$\mathrm{d}\phi = \beta(\mathrm{d}\varepsilon_q)' \tag{10}$$

where l is chosen at any convenient direction to study fabric changes with deformation. Substituting equation (10) in equation (6) results in

$$\mathrm{d}\varepsilon_v = \frac{v_{\mathrm{m}} + \phi v_{\mathrm{m}}}{v_{\mathrm{m}} + \phi v_{\mathrm{m}} - \phi}\left((\mathrm{d}\varepsilon_v)_{\mathrm{m}} + \frac{v_{\mathrm{m}} - 1}{v_{\mathrm{m}} + \phi v_{\mathrm{m}}}\beta(\mathrm{d}\varepsilon_q)'\right) \tag{11}$$

The last expression shows that the volumetric strain increment in structural soils is coupled with the shear strain increment.

ENERGY DISSIPATION

One of the many attractive features of critical state based stress strain models for soils is the rigorous derivation of the yield surface from plastic energy dissipation rather than an apriori assumption of a functional form. Various forms of plastic energy dissipation have been utilized in the past for this purpose.[11–14] In this study, a plastic energy dissipation formulation which includes the effects of soil structure is proposed and used to derive a new yield surface. The new yield surface in turn is used to derive a stress–strain model that accounts for soil fabric.

Consider that a soil specimen deforms with strain increments $((\mathrm{d}\varepsilon_v)_{\mathrm{m}}, \mathrm{d}\varepsilon_q)$ under a stress state (p, q). The external work done per unit volume of the sample due to this process is expressed by:

$$\mathrm{d}W = p(\mathrm{d}\varepsilon_v)_{\mathrm{m}} + q\,\mathrm{d}\varepsilon_q \tag{12}$$

where p and q are the mean stress and deviatoric stress, respectively. For triaxial conditions

$$p = \tfrac{1}{3}(\sigma_1 + 2\sigma_3) \tag{13}$$

$$q = \sigma_1 - \sigma_3 \tag{14}$$

$$(\mathrm{d}\varepsilon_v)_{\mathrm{m}} = \mathrm{d}\varepsilon_1 + 2\mathrm{d}\varepsilon_3 \tag{15}$$

and

$$\mathrm{d}\varepsilon_q = \tfrac{2}{3}(\mathrm{d}\varepsilon_1 - \mathrm{d}\varepsilon_3) \tag{16}$$

in which σ_1 and σ_3 are the major and minor principal stresses, respectively; and ε_1 and ε_3 are the major and minor principal strains, respectively. The corresponding recoverable and irrecoverable external energy, respectively, are

$$\mathrm{d}E = p(\mathrm{d}\varepsilon_v^{\mathrm{e}})_{\mathrm{m}} + q\,\mathrm{d}\varepsilon_q^{\mathrm{e}} \tag{17}$$

and

$$\mathrm{d}D = p(\mathrm{d}\varepsilon_v^{\mathrm{p}})_{\mathrm{m}} + q\,\mathrm{d}\varepsilon_q^{\mathrm{p}} \tag{18}$$

where the superscripts e and p denote the elastic and plastic components. Various assumptions have been made to define the internal incremental energy dissipation dD in relation to the plastic strain increments. At the critical state, $q = Mp$ and $\mathrm{d}\varepsilon_v^{\mathrm{p}} = 0$, and equation (18) reduces to

$$\mathrm{d}D = Mp\,\mathrm{d}\varepsilon_q^{\mathrm{p}} \tag{19}$$

where M is the slope of the critical state line in the p–q diagram. This is the assumption made in the derivation of the cam-clay model.[13] Since wet clay can deform irrecoverably under isotropic stress ($q = 0$), equation (18) becomes

$$(\mathrm{d}D)_{q=0} = p(\mathrm{d}\varepsilon_v^{\mathrm{p}})_{\mathrm{m}} \tag{20}$$

for the condition of isotropic consolidation. Burland[14] proposed a generalization to the internal energy dissipation dD to include this feature as

$$\mathrm{d}D = p\sqrt{(\mathrm{d}\varepsilon_v^{\mathrm{p}})_{\mathrm{m}}^2 + (M\,\mathrm{d}\varepsilon_q^{\mathrm{p}})^2} \tag{21}$$

The volumetric strain increment distribution of structural soils was given by equation (11). Accordingly, the internal energy dissipation of structural soil under isotropic consolidation stress (equation (20)) becomes

$$(\mathrm{d}D)_{q=0} = p\left[\frac{v_{\mathrm{m}} + \phi v_{\mathrm{m}}}{v_{\mathrm{m}} + \phi v_{\mathrm{m}} - \phi}\left((\mathrm{d}\varepsilon_v^{\mathrm{p}})_{\mathrm{m}} + \frac{v_{\mathrm{m}} - 1}{v_{\mathrm{m}} + \phi v_{\mathrm{m}}}\,\beta(\mathrm{d}\varepsilon_q^{\mathrm{p}})'\right)\right] \tag{22}$$

The above relationship indicates that the fabric effects in structural soils will manifest in the form of shear volume coupling in the internal energy dissipation. The relationship can be simplified with the use of a coupling parameter, α':

$$(\mathrm{d}D)_{q=0} = p[(\mathrm{d}\varepsilon_v^{\mathrm{p}})_{\mathrm{m}} + \alpha'(\mathrm{d}\varepsilon_q^{\mathrm{p}})'] \tag{23}$$

where the value of α' can be obtained by equating equations (22) and (23).

The contribution of plastic shear strain increment in l-direction to the energy dissipation is expressed in terms of the plastic shear strain increment in a triaxial cell by

$$\alpha'(\mathrm{d}\varepsilon_q^{\mathrm{p}})' = \alpha\,\mathrm{d}\varepsilon_q^{\mathrm{p}} \tag{24}$$

Consequently, equation (23) becomes

$$(\mathrm{d}D)_{q=0} = p[(\mathrm{d}\varepsilon_v^{\mathrm{p}})_{\mathrm{m}} + \alpha\,\mathrm{d}\varepsilon_q^{\mathrm{p}}] \tag{25}$$

The new expression for internal dissipation at the isotropic consolidation state and the expression for internal dissipation at the critical state (equation (19)) can be generalized following Burland:[14]

$$\mathrm{d}D = p\sqrt{((\mathrm{d}\varepsilon_v^{\mathrm{p}})_{\mathrm{m}} + \alpha\,\mathrm{d}\varepsilon_q^{\mathrm{p}})^2 + (M\,\mathrm{d}\varepsilon_q^{\mathrm{p}})^2} \tag{26}$$

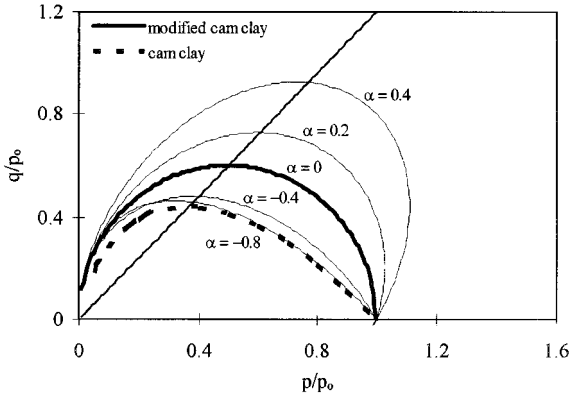

Figure 2. The change in shape of the yield surface with the fabric parameter

Combining the above expression with that of the external irrecoverable energy (equation (18)) results in

$$\psi = \frac{(\mathrm{d}\varepsilon_v^{\mathrm{p}})_{\mathrm{m}}}{\mathrm{d}\varepsilon_q^{\mathrm{p}}} = \frac{M^2 + \alpha^2 - \eta^2}{2(\eta - \alpha)} \tag{27}$$

where $\eta = q/p$, and ψ is the plastic strain increment ratio. It is noted that α varies with deformation. However, as discussed later, the soil deformation is considered in two main regions where constant values of α are assumed. The equation of the current yield locus is obtained by:[15]

$$\ln\left(\frac{p_0}{p}\right) = \int_{\eta_{\mathrm{in}}}^{\eta} \frac{\mathrm{d}\eta}{\psi + \eta} \tag{28}$$

to get

$$\frac{p}{p_0} = \left[\frac{M^2 + (\eta_{\mathrm{in}} - \alpha)^2}{M^2 + (\eta - \alpha)^2}\right] \tag{29}$$

where η_{in} is the initial value of q/p, and p_0 is the value of p when $\eta = \eta_{\mathrm{in}}$. For isotropically consolidated samples, use of $\eta_{\mathrm{in}} = 0$ results in

$$\frac{p}{p_0} = \left[\frac{M^2 + \alpha^2}{M^2 + (\eta - \alpha)^2}\right] \tag{30}$$

The general shape of the new yield surface consists of a rotated and distorted ellipse, which is similar to the yield surface proposed by Dafalias.[11] The change in shape of the yield surface with the fabric coupling parameter α is shown in Figure 2. The figure also shows the yield surfaces for the family of cam clay models. The surface reduces to the modified cam clay yield surface for $\alpha = 0$ and approaches the cam clay yield surface at negative values of α. For natural soils, the initial values of p_0 and η will be at the intersection of the K_0 line and the line yield surface. For the special case of a K_0 normally consolidated soil, these values become $p_{K_0} = \sigma_1(1 + 2K_0)/3$ and $\eta_{K_0} = 3(1 - K_0)/(1 + 2K_0)$.

Note that for non-zero values of α the yield surface may not be normal to the p/p_0 axis. This will result in the development of both volumetric and shear plastic strain increments for hydrostatic

pressure changes along the p-axis. The shear strain increment is the result of the coupling due to changes in fabric during this loading (see equations (22) and (23)).

SOIL PLASTICITY MODEL

The soil is assumed to obey the associated flow rule in the strain-hardening region. The plastic potentials, g, are given by the same equation for the family of the yield loci, f, :

$$g = f = \frac{M^2 + (\eta_{\text{in}} - \alpha)^2}{M^2 + (\eta - \alpha)^2} - \frac{p}{p_0} \tag{31}$$

The differential form of the yield loci is

$$\frac{\partial f}{\partial p'} \mathrm{d}p' + \frac{\partial f}{\partial q} \mathrm{d}q + \frac{\partial f}{\partial p'_0} \mathrm{d}p'_0 = 0 \tag{32}$$

The plastic strain increments form a mechanism of plastic deformation related to the normal to the plastic potential at the current effective stress state so that

$$(\mathrm{d}\varepsilon_v^{\mathrm{p}})_{\mathrm{m}} = \chi \partial p / \partial p \tag{33}$$

and

$$\mathrm{d}\varepsilon_q^{\mathrm{p}} = \chi \partial f / \partial q \tag{34}$$

where χ is a scalar multiplier whose value will be derived subsequently from the assumed hardening characteristics of the soil.

The change in the size of the yield loci, that is the change in p_0, is linked with increments of both plastic volumetric strain and plastic shear strain following a hardening rule:

$$\mathrm{d}p_0 = \frac{\partial p_o}{(\partial \varepsilon_v^{\mathrm{p}})_{\mathrm{m}}} (\mathrm{d}\varepsilon_v^{\mathrm{p}})_{\mathrm{m}} + \frac{\partial p_0}{\partial \varepsilon_q^{\mathrm{p}}} \mathrm{d}\varepsilon_q^{\mathrm{p}} \tag{35}$$

Combining equations (32)–(35) yields an expression for the scalar multiplier χ:

$$\chi = - \frac{\left[\dfrac{\partial f}{\partial tp} \mathrm{d}p + \dfrac{\partial f}{\partial q} \mathrm{d}q \right]}{\dfrac{\partial f}{\partial p_0} \left[\dfrac{\partial p_0}{(\partial \varepsilon_v^{\mathrm{p}})_{\mathrm{m}}} \dfrac{\partial f}{\partial p} + \dfrac{\partial p_0}{\partial \varepsilon_q^{\mathrm{p}}} \dfrac{\partial f}{\partial q} \right]} \tag{36}$$

In order to utilise χ, each of its components must be determined. The change in the isotropic plastic specific volume can be shown to be:[16]

$$\Delta v_{\mathrm{m}}^{\mathrm{p}} = - (\lambda_{\mathrm{m}} - \kappa_{\mathrm{m}}) \ln \frac{p_{02}}{p_{01}} \tag{37}$$

where λ_{m} and κ_{m} are the isotropic compression and swelling indices, respectively, and p_{02} and p_{01} are two normalizing stresses (Figure 3 plane II). The general swelling and compression indices accounting for soil fabric can be shown to be, respectively:

$$\kappa = \kappa_{\mathrm{m}}(1 + \phi) - p \frac{\partial \phi}{\partial p} (v_{\mathrm{m}} - 1) \tag{38}$$

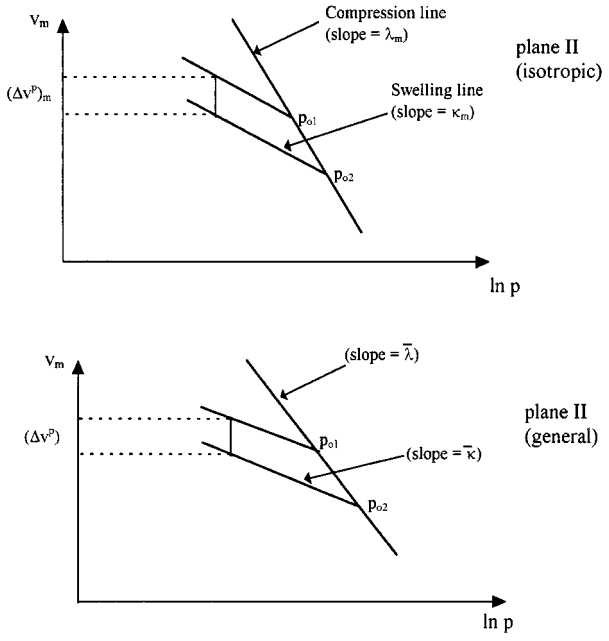

Figure 3. Schematic of the change in specific volume

and

$$\lambda = \lambda_{\mathrm{m}}(1 + \phi) - p\frac{\partial \phi}{\partial p}(v_{\mathrm{m}} - 1) \tag{39}$$

In spite of the small fluctuations of λ and κ with fabric changes, the effect of fabric is assumed to follow a certain trend that allows the average values, $\bar{\lambda}$ and $\bar{\kappa}$, to be obtained from equations (38) and (39) with an average value of fabric $\bar{\phi}$. These values will generally be different from the isotropic values (λ_{m} and κ_{m}).

Following the derivation of equation (37), the change in the general plastic specific volume can be shown to be (Figure 3 plane I):

$$\Delta v^{\mathrm{p}} = -(\bar{\lambda} - \bar{\kappa}) \ln \frac{p_{02}}{p_{01}} \tag{40}$$

In the limit, the above equation reduces to

$$(\mathrm{d}\varepsilon_v^{\mathrm{p}})_{\mathrm{m}} + \alpha\, \mathrm{d}\varepsilon_q^{\mathrm{p}} = (\bar{\lambda} - \bar{\kappa})\frac{\mathrm{d}p_0}{vp_0} \tag{41}$$

Combining the new expressions of $\bar{\lambda}$ and $\bar{\kappa}$ with the above equation results in:

$$(\mathrm{d}\varepsilon_v^{\mathrm{p}})_{\mathrm{m}} + \alpha\, \mathrm{d}\varepsilon_q^{\mathrm{p}} = (\lambda_{\mathrm{m}} - \kappa_{\mathrm{m}})\frac{\mathrm{d}p_0}{v_{\mathrm{m}}p_0} + \frac{\bar{\phi}(\lambda_{\mathrm{m}} - \kappa_{\mathrm{m}})}{v_{\mathrm{m}} + \bar{\phi}v_{\mathrm{m}} - \bar{\phi}v_{\mathrm{m}}}\frac{\mathrm{d}p_0}{v_{\mathrm{m}}\, p_0} \tag{42}$$

The isotropic plastic volumetric strain increment is

$$(\mathrm{d}\varepsilon_v^{\mathrm{p}})_{\mathrm{m}} = (\lambda_{\mathrm{m}} - \kappa_{\mathrm{m}})\frac{\mathrm{d}p_0}{v_{\mathrm{m}}p_0} \tag{43}$$

which can be rearranged to give

$$\frac{\partial p_0}{(\partial\varepsilon_v^{\mathrm{p}})_{\mathrm{m}}} = \frac{v_{\mathrm{m}}p_0}{(\lambda_{\mathrm{m}} - \kappa_{\mathrm{m}})} \tag{44}$$

Subtracting equation (43) from equation (42) and rearranging results in:

$$\frac{\partial p_0}{\partial\varepsilon_q^{\mathrm{p}}} = \frac{\alpha v_{\mathrm{m}}(v_{\mathrm{m}} + \bar{\phi}v_{\mathrm{m}} - \bar{\phi})}{\bar{\phi}(\lambda_{\mathrm{m}} - \kappa_{\mathrm{m}})}p_0 = \gamma\frac{v_{\mathrm{m}}p_0}{(\lambda_{\mathrm{m}} - \kappa_{\mathrm{m}})} \tag{45}$$

where $\gamma = \alpha(v_{\mathrm{m}} + \bar{\phi}v_{\mathrm{m}} - \bar{\phi})/\bar{\phi}$. The derivation of equation (31) results in the components for

$$\frac{\partial f}{\partial p} = \frac{M^2 - \eta^2 + \alpha^2}{M^2 + (\eta - \alpha)^2}\frac{1}{p} \tag{46}$$

$$\frac{\partial f}{\partial q} = \frac{\eta - \alpha}{M^2 + (\eta - \alpha)^2}\frac{2}{p} \tag{47}$$

and

$$\frac{\partial f}{\partial p_0} = -\frac{1}{p_0} \tag{48}$$

Substituting equations (44)–(48) into equation (36) and combining the result with equations (33)–(34), the strain increments can be expressed in terms of the mean stress, and deviatoric stress increments. The resulting plastic stress–strain response can be summarized in a matrix form:

$$\begin{bmatrix}(\mathrm{d}\varepsilon_v^{\mathrm{p}})_{\mathrm{m}}\\ \mathrm{d}\varepsilon_q^{\mathrm{p}}\end{bmatrix} = \frac{(\lambda_{\mathrm{m}} - \kappa_{\mathrm{m}})(M^2 - \eta^2 + \alpha^2)}{pv_{\mathrm{m}}(M^2 + (\eta - \alpha)^2)\,((M^2 - \eta^2 + \alpha^2) + 2\gamma(\eta - \alpha))} \times \begin{bmatrix} M^2 - \eta^2 + \alpha^2) & 2(\eta - \alpha)\\ 2(\eta - \alpha) & \dfrac{4(\eta - \alpha)^2}{(M^2 - \eta^2 + \alpha^2)}\end{bmatrix}\begin{bmatrix}\mathrm{d}p\\ \mathrm{d}q\end{bmatrix} \tag{49}$$

BEHAVIOR OF STRUCTURAL SOILS

The critical state idealization envisages the shear stress–strain curve for all reconstituted clays as rising smoothly to a plastic failure. Natural soils, however, are more sensitive and brittle than reconstituted materials and in most cases strain-soften to failure. The strain-softening behaviour becomes more pronounced as the skeletal nature of structure increases. This general behaviour can be interpreted by suggesting that soils with collapsible structure attain an apparent critical state at which the solid skeleton collapses. In the case of a specimen without collapsible structure, the collapse and critical states coincide at the moment of plastic failure. The behaviour of such soils is governed entirely by the equations derived for the hardening region. On the contrary, a soil whose collapse state precedes the true critical state, will tend towards a false critical state (Figure 4, point A). Once the structure begins to collapse, the position of the true critical state

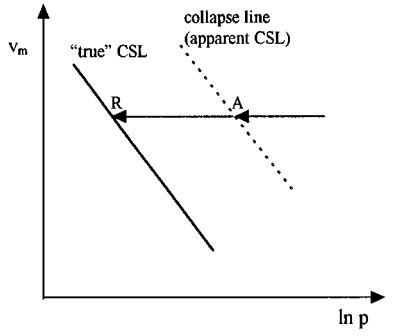

Figure 4. Illustration of collapse and critical state

becomes evident and the soil will approach the critical state line (Figure 4, point R). This means that this type of soil existed in some unusual or meta-stable configuration. The detailed description of the collapse behaviour can also be illustrated in the normalized q–p plane.[7]

The effects of structure are expected to be reflected in the initial stages of the deformation. Therefore, in the proposed model the pre-collapse region is described by the set of equations derived for the strain-hardening material. When the structural effects cease to contribute to internal dissipation, the value of α reduces to zero and the formulations reduce to those of modified cam clay.[15] In the post-collapse or strain softening region, the volumetric strain decreases (i.e. the yield surface shrinks with loading), while the shear strain increases rapidly resulting in a negative volumetric to shear strain increment ratio. This ratio is assumed to be equivalent to that in the pre-collapse region (equation (27)) but with an opposite sign. The corresponding plastic potential function is obtained from equation (28).

Note that α (equation (26)) is dependent on both the initial state and variation of fabric, and its value in equations (29) and (30) changes at each infinitesimal increment. In practice, however, the fabric variation is very small comparing to its initial state until a sudden collapse of the skeleton occurs. Thus the collapse state is considered to divide the deformation into two distinct regions. Consequently, the complete yield surface for structural soils can be captured by constant values of α in these two regions.

The solid skeleton of structural soils is expected to provide the full critical state energy dissipation in the initial stages of deformation. The soil will be in a transition state in the post-collapse region where it can be expected to mobilize only part of its full capacity. To capture this, the shear stress ratio parameter M in the dissipation equation (equation (26)) is changed to a new value N. The value of N will be less than or equal to M and may even be quite small depending on a number of factors, including material characteristics, loading rate, and drainage conditions.

The magnitude of the new normalizing mean stress, p_0 (equation (28)) is also dependent on soil structure. This can be best illustrated by observing the soil behaviour in the compression plane (Figure 5). Plane (I) shows the general specific volume (v) versus the mean stress (p) . When the effects of fabric are neglected it reduces to plane (II) with isotropic specific volume (v_m) as the ordinate. Consequently, plane (I) governs the actual soil behaviour with fabric changes, while plane (II) represents the average quantities measured in the lab and used in many of the current isotropic models. Suppose that a soil specimen is subjected to undrained loading. The value of the specific volume, v (plane I), can be greater or less than the isotropic value, v_m (plane II) depending

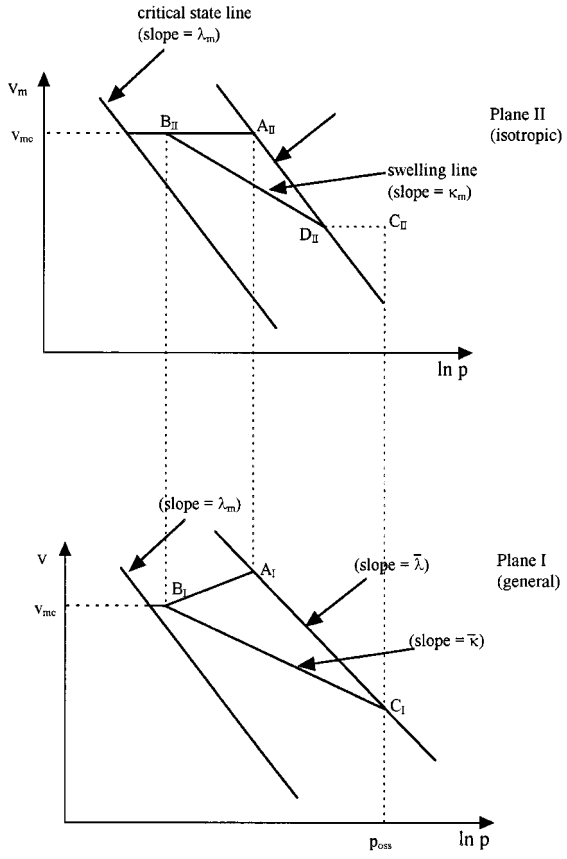

Figure 5. Definition of the normalizing mean stress

on the state of initial fabric arrangement. The initial value of the normalizing mean stress, p_0, is controlled by the experiment, and is the same in both planes (points A_I and A_{II}). When the specimen is sheared, fabric is disturbed, and the specimen will head towards the isotropic specific volume, v_{mc} (points B_I and B_{II}). Changes in fabric arrangement during deformation will cause fluctuations of the specific volume around a trend line ($A_I B_I$) . Therefore, the undrained stress path in plane (I) need not be horizontal as in plane (II). At the moment of collapse (point B_I), the specimen identifies p_{oss} (point C_I) as its normalizing mean stress, and as the fabric is destroyed, the behaviour is governed by plane (II). The sample, however, continues to identify p_{oss} as its new normalizing mean stress (point C_{II}), which is higher, for this case, than its value when the effects of fabric are neglected (point D_{II}). Consequently, softening takes place and p_{oss} decreases significantly. The value of p_{oss} can be evaluated by equating the value of p at the collapse state on the yield surface (equation (28)) from the pre-collapse segment to that of the post-collapse segment:

$$p_{oss} = p_0 \left[\frac{(M^2 + (\eta_{in} - \alpha)^2)(N^2 + \eta_{ss}^2)}{(M^2 + (\eta_{ss} - \alpha)^2)(N^2 + \eta_{in}^2)} \right] \tag{50}$$

where η_{ss} is the stress ratio at the collapse state.

As pointed out earlier in this paper the compression and swelling indices in plane I ($\bar{\lambda}$ and $\bar{\kappa}$) will be different from those in plane II (λ_m and κ_m). The critical state line, however, has the same slope in both planes since specimens at this line are assumed to have no fabric effects associated with them. Therefore, in general the compression and critical state lines are not parallel in plane I.

APPLICATIONS

A previous study by the same authors[7] has shown that the proposed synthesis is satisfactory in modeling the experimental yield and state boundary surfaces for a number of soils. In the current study, the new synthesis has been used to model the stress–strain behaviour. In the plastic region (post-yield), the total stress–strain response is modelled with the plastic strain increments. The elastic contribution is neglected as it is very small compared to the plastic contribution.

Atkinson *et al.*[17] presented results of a series of triaxial tests performed to investigate the strength and state boundary surface of K_0 normally consolidated kaolin clay. These tests were comprised of a variety of stress and strain controlled loading paths including drained, constant p, and undrained tests in compression and extension. Figures 6–13 show a comparison between the shear stress–shear strain and volumetric strain–shear strain curve predictions by the proposed model (equation 49), the modified cam clay model, and the experimental data. The relevant model parameters used in the prediction are presented in Table I. In all of these tests, softening behaviour was not observed and the stress–strain relation is captured by equations (23)–(49). The stress–strain predictions of the proposed model and modified cam clay compare well with the former being more closer to the experimental data. The proposed model, however, is superior in modelling the volumetric strain–shear strain behaviour as shown in Figures 7, 9, 11, and 13. Figures 14–16 show the shear stress–shear strain curves for a group of extension triaxial tests on

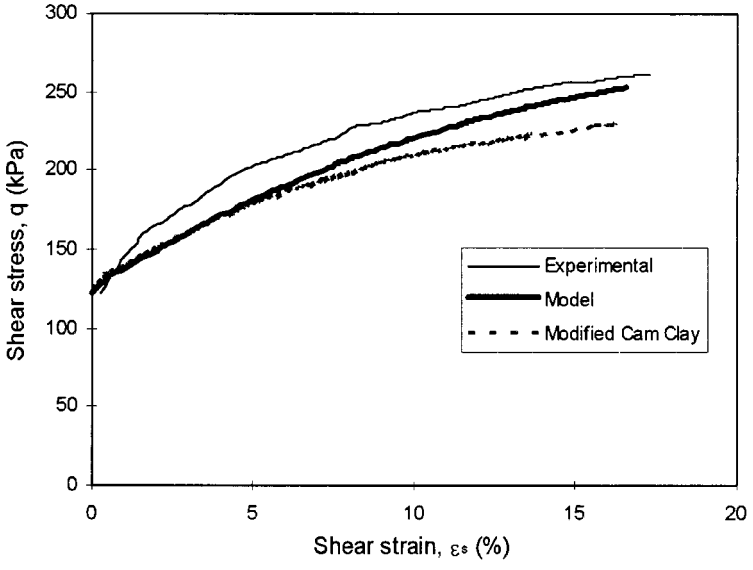

Figure 6. Shear stress–shear strain curve for anisotropic drained compression triaxial test (data from Reference 17)

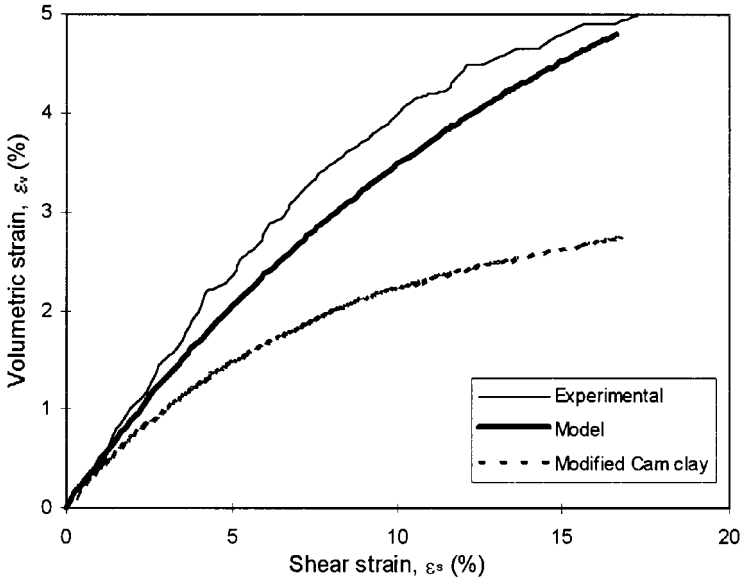

Figure 7. Volumetric strain during shearing for anisotropic drained compression triaxial test (data from Reference 17)

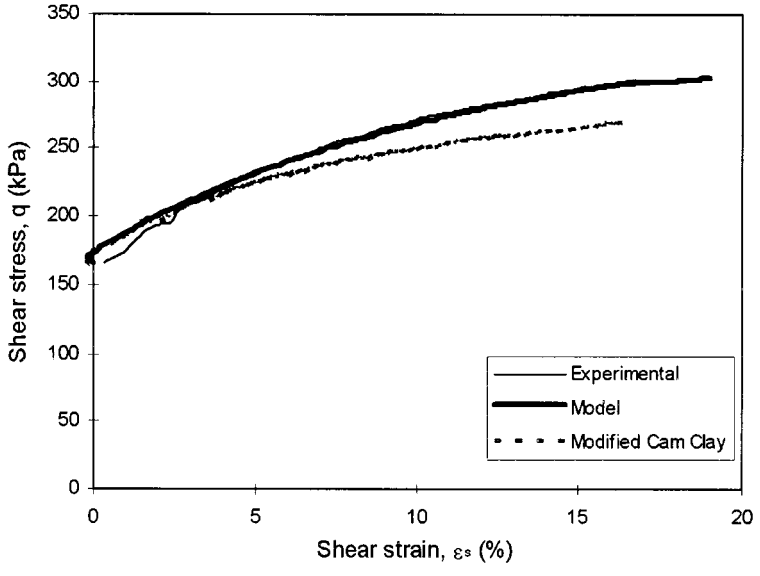

Figure 8. Shear stress–shear strain curve for anisotropic drained compression triaxial test (data from Reference 17)

anisotropic consolidated samples. The predictions show that the model is quite good in capturing the extension behaviour of these specimens.

Figures 17 and 18 present a comparison of the stress–strain curves by the present model and the modified cam clay with the experimental data of isotropic consolidated triaxial compression

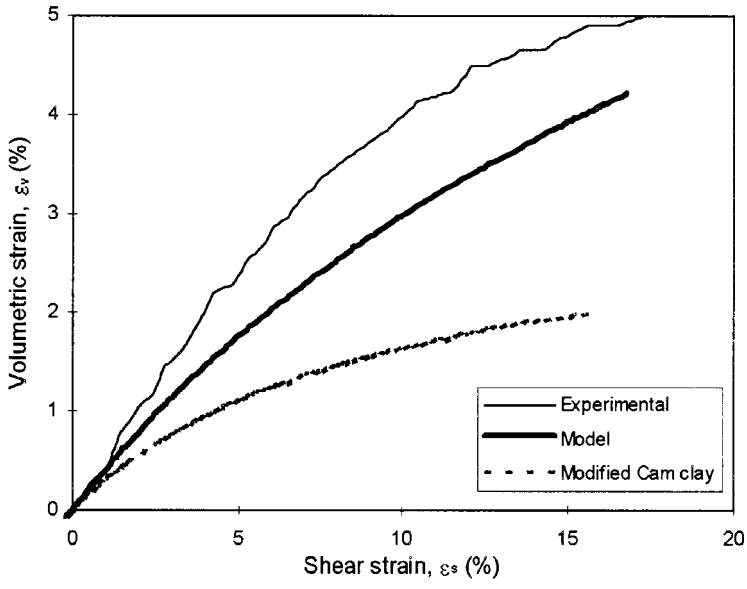

Figure 9. Volumetric strain during shearing for anisotropic drained compression triaxial test (data from Reference 17)

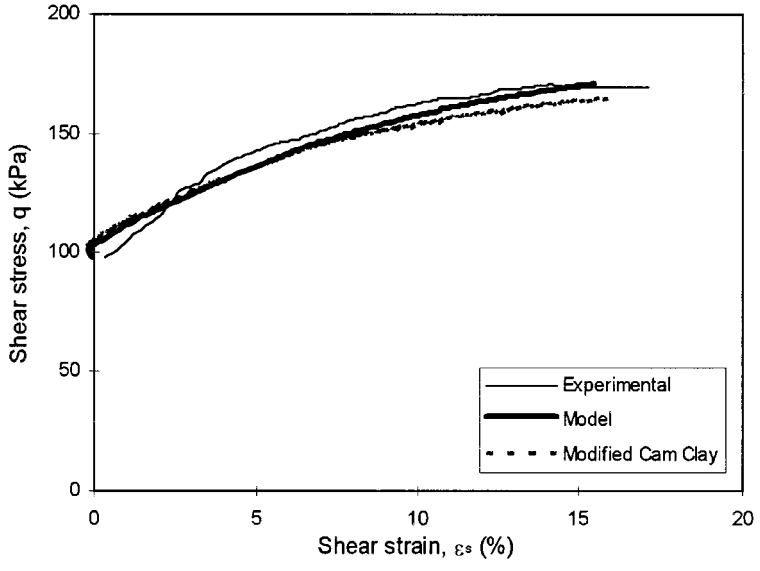

Figure 10. Shear stress–shear strain curve for anisotropic compression triaxial test with constant mean stress (data from Reference 17)

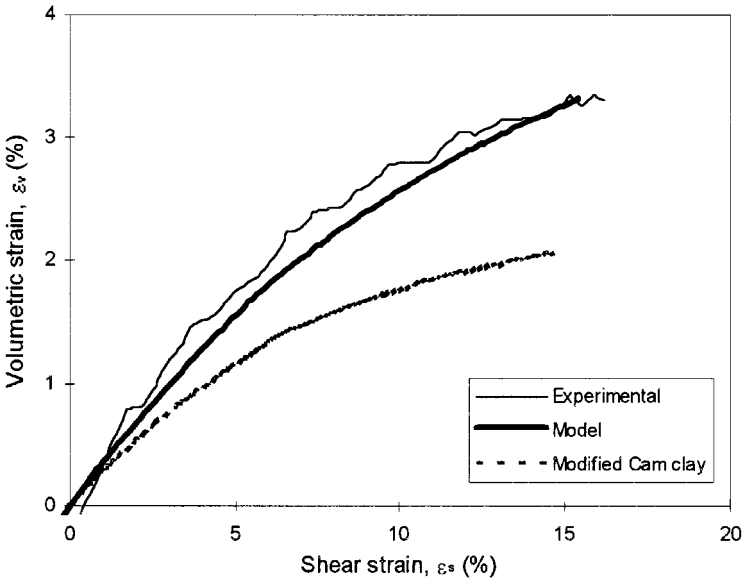

Figure 11. Volumetric strain during shearing for anisotropic compression triaxial test with constant mean stress (data from Reference 17)

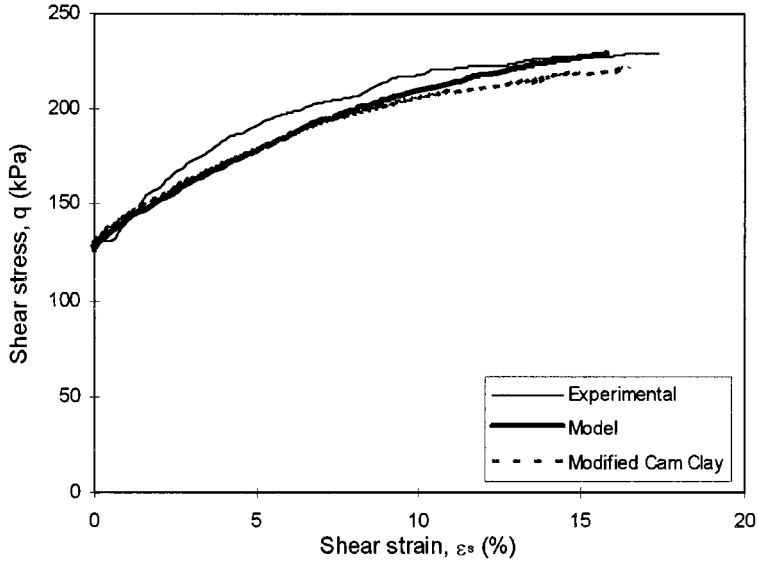

Figure 12. Shear stress–shear strain curve for anisotropic compression triaxial test with constant mean stress (data from Reference 17)

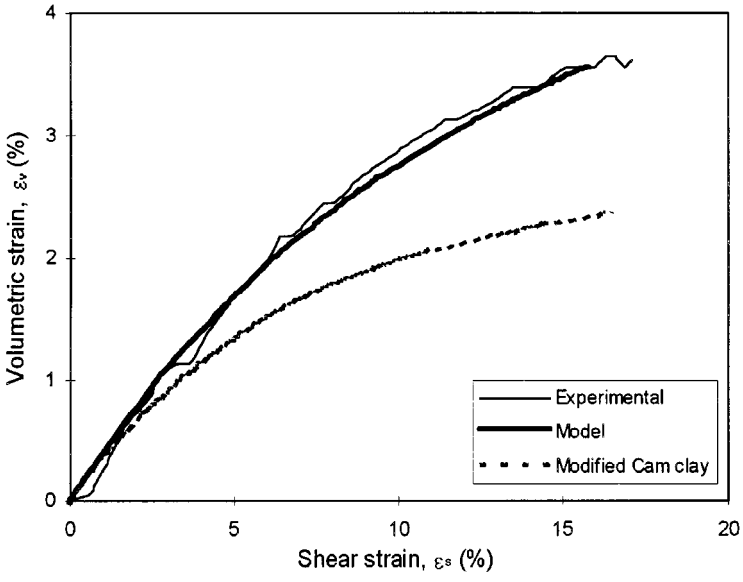

Figure 13. Volumetric strain during shearing for anisotropic compression triaxial test with constant mean stress (data from Reference 17)

Table I. Relevant equations based on critical state concept

	Cam-clay	Modified cam-clay	New model
Dissipation energy increment	$\mathrm{d}D = Mp\,\mathrm{d}\varepsilon_q^{\mathrm{p}}$	$\mathrm{d}D = p\sqrt{(\mathrm{d}\varepsilon_v^{\mathrm{p}})^2 + (M\,\mathrm{d}\varepsilon_q^{\mathrm{p}})^2}$	$\mathrm{d}D = p\sqrt{(\mathrm{d}\varepsilon_v^{\mathrm{p}} + \alpha\,\mathrm{d}\varepsilon_q^{\mathrm{p}})^2 + (M\,\mathrm{d}\varepsilon_q^{\mathrm{p}})^2}$
Plastic strain increment ratio	$\Psi = \dfrac{\mathrm{d}\varepsilon_v^{\mathrm{p}}}{\mathrm{d}\varepsilon_q^{\mathrm{p}}} = M - \eta$	$\Psi = \dfrac{\mathrm{d}\varepsilon_v^{\mathrm{p}}}{\mathrm{d}\varepsilon_q^{\mathrm{p}}} = \dfrac{M^2 - \eta^2}{2\eta}$	$\Psi = \dfrac{\mathrm{d}\varepsilon_v^{\mathrm{p}}}{\mathrm{d}\varepsilon_q^{\mathrm{p}}} = \dfrac{M^2 + \alpha^2 - \eta^2}{2(\eta - \alpha)}$
Yield surface	$\eta = M \ln\left(\dfrac{p_0}{p}\right)$	$\dfrac{p}{p_0} = \left(\dfrac{M^2}{M^2 + \eta^2}\right)$	$\dfrac{p}{p_0} = \left(\dfrac{M^2 + (\eta_{\mathrm{in}} - \alpha)^2}{M^2 + (\eta - \alpha)^2}\right)$

and extension tests on Lower Cromer Till presented by Gens.[18] Lower Cromer Till is a low plasticity clay. The parameters used in modelling are shown in Table I. The two models show a good agreement with the current model plotting closer to the experimental values. Figure 19 shows that the model fits very well with the experimental values of anisotropic consolidated undrained triaxial extension test. Figure 20 shows the softening behaviour associated with the anisotropic undrained compression triaxial test and the model. The complete stress–strain curve was captured by two expressions for each of the yield surface and the plastic potential function. The pre-collapse region was modelled using equation (29) for both the yield surface and plastic potential function (i.e. equations (33)–(49) were used directly in modelling this portion). The hardening behaviour is very small in this case. The softening behaviour, however, was modelled

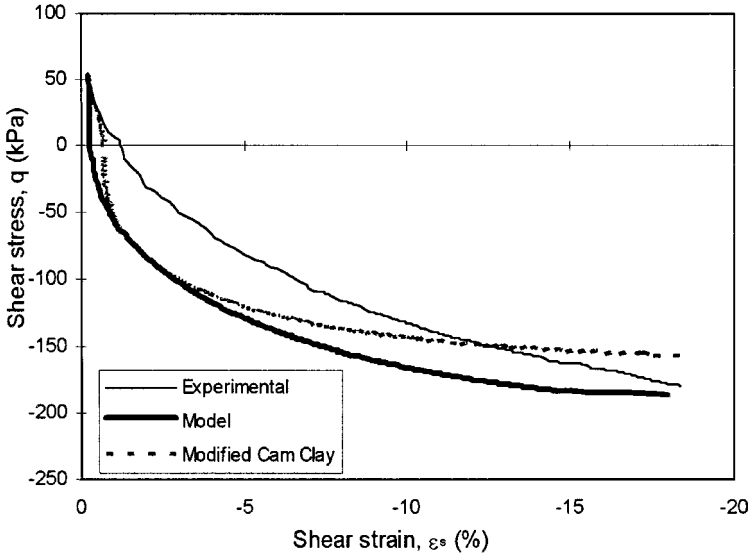

Figure 14. Shear stress–shear strain curve for anisotropic extension triaxial test with constant mean stress (data from Reference 17)

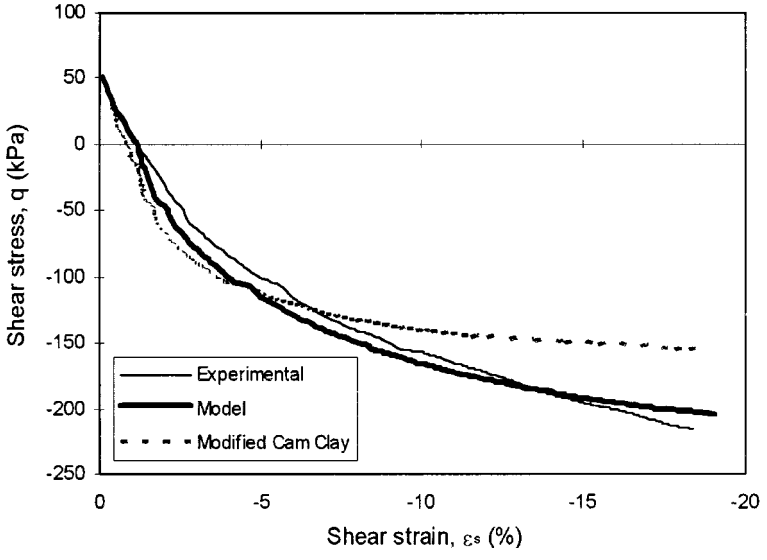

Figure 15. Shear stress–shear strain curve for anisotropic extension triaxial test with constant mean stress (data from Reference 17)

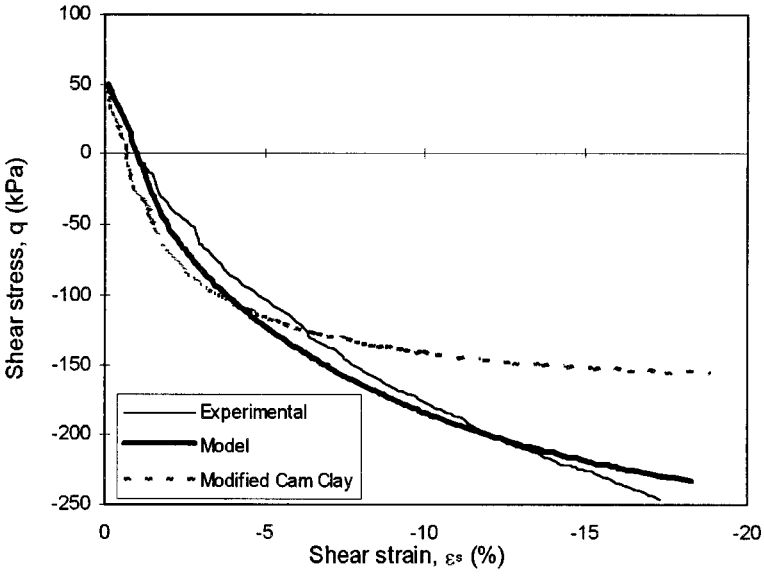

Figure 16. Shear stress–shear strain curve for anisotropic extension triaxial test with constant mean stress (data from Reference 17)

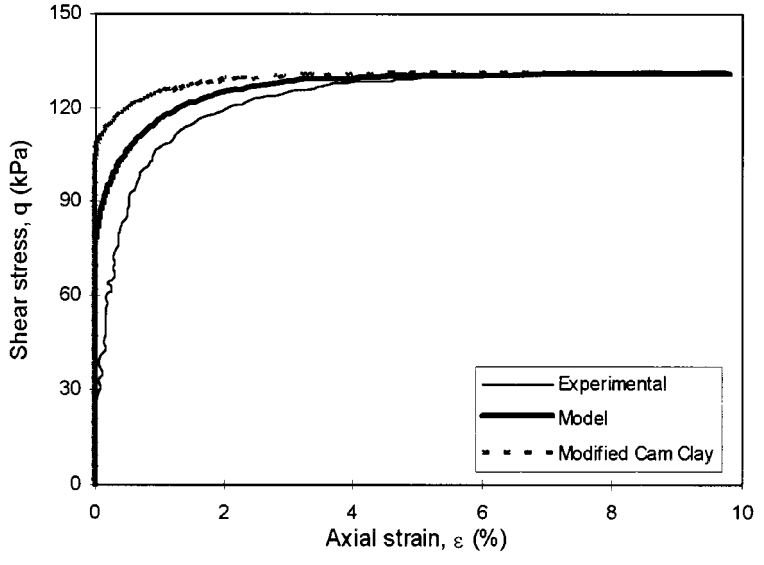

Figure 17. Shear stress–shear strain curve for isotropic undrained compression triaxial test (data from Reference 18)

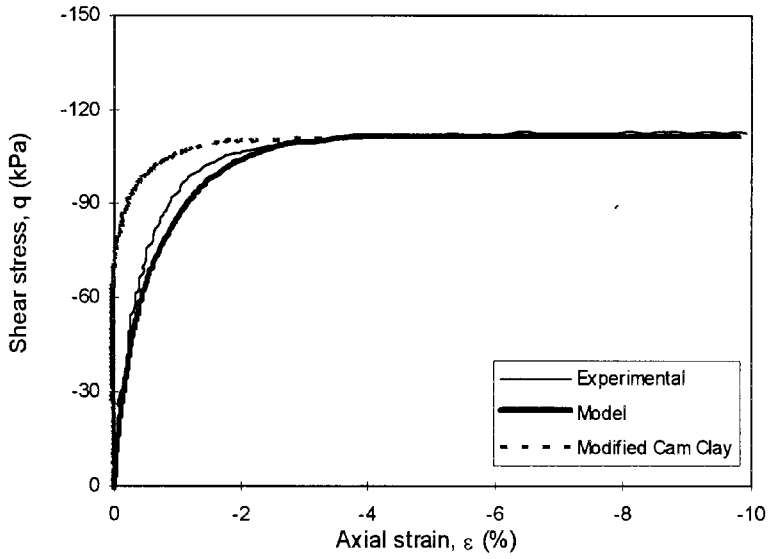

Figure 18. Shear stress–shear strain curve for isotropic undrained extension triaxial test (data from Reference 18)

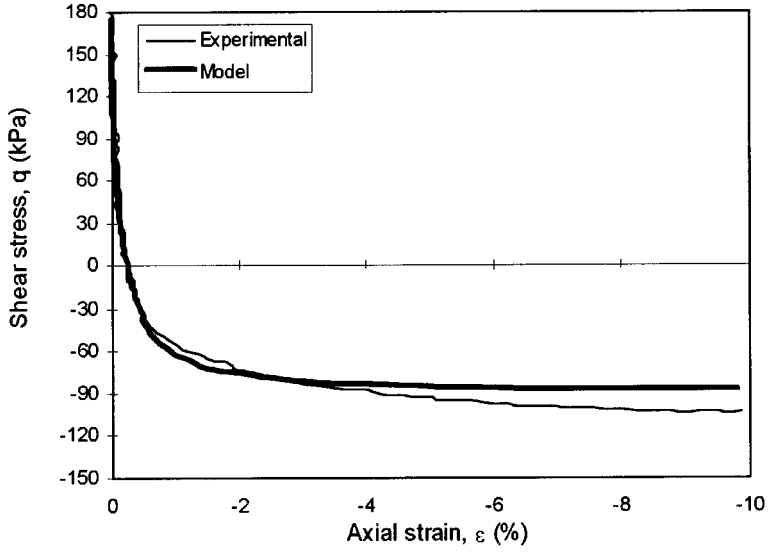

Figure 19. Shear stress–shear strain curve for anisotropic undrained extension triaxial test (data from Reference 18)

with $\alpha = 0$ and $p_0 = p_{oss}$ in equation (29) for the yield surface, while the plastic potential was taken by substituting equation (27) with an opposite sign, as explained previously, into equation (28). Equations (33)–(49) were adjusted subsequently for the latter yield surface and plastic potential function and used to model the softening region.

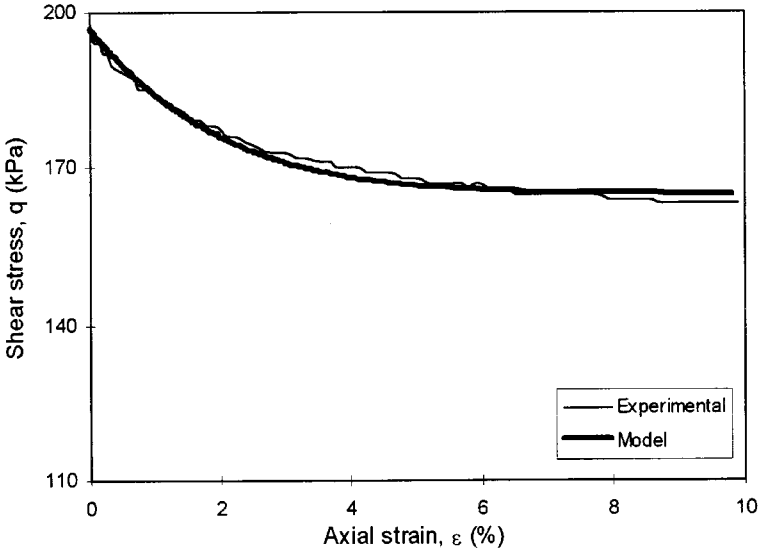

Figure 20. Shear stress–shear strain curve for anisotropic undrained compression triaxial test (data from Reference 18)

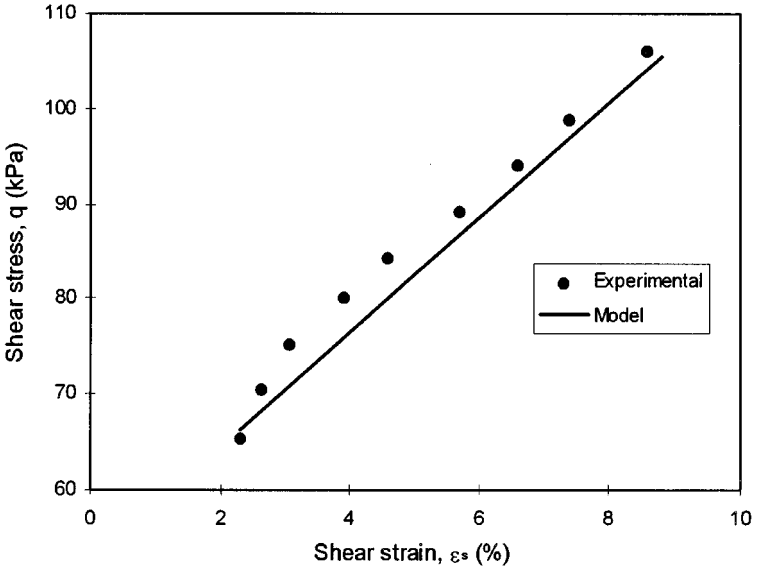

Figure 21. Shear stress–shear (post-yield) curve for drained compression triaxial test of natural clay (data from Reference 4)

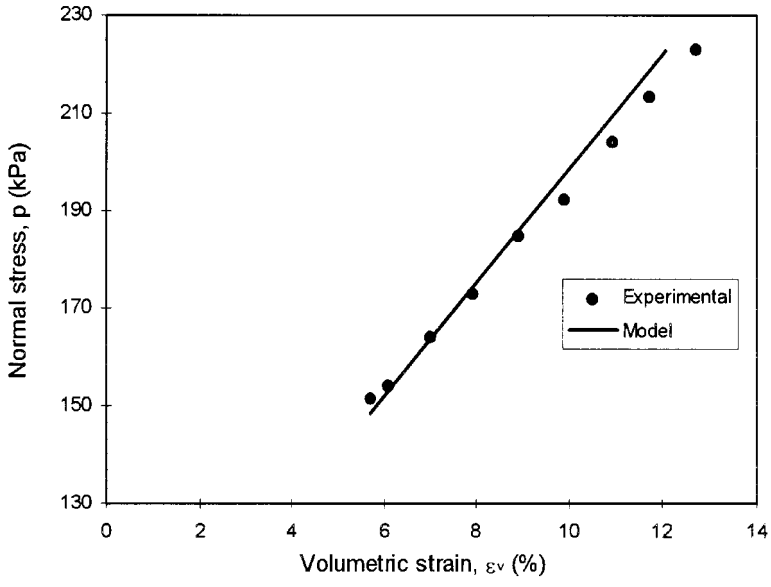

Figure 22. Normal stress–volumetric strain (post-yield) curve for drained compression triaxial test of natural clay (data from Reference 4)

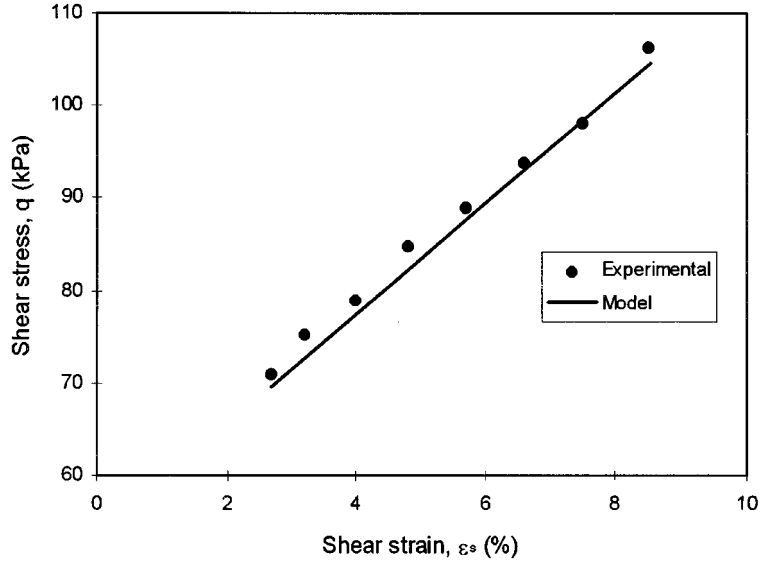

Figure 23. Shear stress–shear strain (post-yield) curve for drained compression triaxial test of natural clay (data from Reference 19)

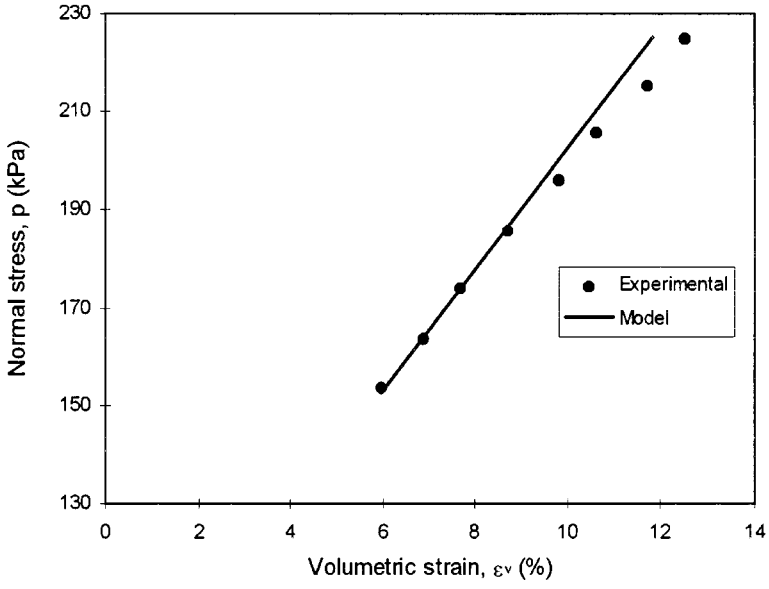

Figure 24. Normal stress–volumetric strain (post-yield) curve for drained compression triaxial test of natural clay (data from Reference 19)

Tests on remolded clays and normally consolidated natural clays emphasize the non-linearity of clay behaviour. Under certain circumstances, however, clays can show a stiffer and more linear response over a limited range of stresses in the post-yield region than suggested by the classical cam clay models.[19] This has been confirmed by laboratory tests on specimens which have been carefully sampled and trimmed to preserve the *in situ* soil fabric.[4,20] Graham *et al.*[5] presented test results on Winnipeg clay in Canada that showed linear behaviour in both the pre- and post-yield regions. The pre-yield behaviour can be predicted satisfactorily by the linear isotropic elasticity. This region, hence, is not presented here and the post-yield behaviour is modelled in Figures 21–24. The relevant model parameters used in the modeling are shown in Table II.

CONCLUSIONS

A new model to incorporate the effects of fabric on the behaviour of soils is put forward. The porosity of these soils is considered to be a directional measure and its distribution is characterized by a functional form. The energy dissipation formulation of the critical state soil mechanics has been modified to incorporate the effects of fabric. The new formulation was used to derive expressions for the yield locus and plastic stress–strain behaviour of soils. The yield surfaces of the current family of cam clay models result as special cases of the new model.

The case studies on a number of soils have shown that the model is able to capture many of the features associated with their deformation. The soils consisted of laboratory isotropically consolidated clays, K_0 consolidated clays, and natural clays. The advantage of the new model is very well identified in modeling K_0 consolidated and natural soils. It was shown that the

Table II. Model parameters for experimental data

Source	Figure	M	N	α	γ
Reference 17, Figure 2, Test C2	6	0·85	0·85	− 0·165	− 0·090
Reference 17, Figure 5(a), Test C2	7	0·85	0·85	− 0·165	− 0·090
Reference 17, Figure 2, Test C3	8	0·85	0·85	− 0·100	− 0·060
Reference 17, Figure 5(a), Test C3	9	0·85	0·85	− 0·100	− 0·060
Reference 17, Figure 3, Test C4	10	0·85	0·85	− 0·165	− 0·090
Reference 17, Figure 5(b), Test C4	11	0·85	0·85	− 0·165	− 0·090
Reference 17, Figure 3, Test C5	12	0·85	0·85	− 0·100	− 0·060
Reference 17, Figure 5(b), Test C5	13	0·85	0·85	− 0·100	− 0·060
Reference 17, Figure 3, Test E2	14	0·85	0·85	− 0·100	− 0·090
Reference 17, Figure 3, Test E3	15	0·85	0·85	− 0·150	− 0·120
Reference 17, Figure 3, Test E4	16	0·85	0·85	− 0·200	− 0·170
Reference 18, Figure 6(20), Test IC2-1	17	1·20	1·20	− 0·500	− 0·580
Reference 18, Figure 6(42), Test IE-1	18	0·85	0·85	0·300	0·310
Reference 18, Figure 6(94), Test AE-1	19	0·85	0·85	0·900	1·340
Reference 18, Figure 6(64), Test AC2-1	20	1·20	0·88	0·500*	0·700*
Reference 4, Figure 2, Test T312	21	0·668	0·668	0·330	− 0·220
Reference 4, Figure 2, Test T312	22	0·668	0·668	0·330	− 0·220
Reference 19, Figure 2, Test T313	23	0·668	0·668	0·330	− 0·220
Reference 19, Figure 2, Test T313	24	0·668	0·668	0·330	− 0·220

* Pre-collapse value.

strain-softening behaviour of some soils initiates after the collapse of the meta-stable skeleton. The collapse is identified in terms of the change in the initial values of the key model parameters, namely the fabric parameter α, the new normalizing mean stress p_0, and the shear stress ratio M or N. The behaviour subsequent to collapse is highly unstable and depends on a number of factors that affect the mobilization of N. These include the rate of loading, the collapsiveness of the solid skeleton, and the drainage conditions. The post-yield linearity which comes from a wide variety of lightly overconsolidated or cemented clays was captured quite well with the presented model.

In the analysis of the test data, the α parameter was chosen to fit the experimental data, however, it is preferable to verify its value from microscopic observations. This is currently under investigation.

ACKNOWLEDGEMENTS

The work presented in this paper is part of a research program supported by the National Science Foundation under the grants of CMS-9304506 and CMS-9309345 awarded to Washington State University and the Georgia Institute of Technology.

REFERENCES

1. J. K. Mitchell, *Fundamentals of Soil Mechanics*, Wiley, New York, 1993.
2. S. Leroueil, P. R. Vaughan, 'The general and congruent effects of structure in natural soils and weak rocks', *Geotechnique*, **40,** 467–488 (1990)

3. J. B. Burland, 'On the compressibility and shear strength of natural clays', *Geotechnique*, **40,** 329–378 (1990).
4. J. Graham, M. L. Noonan and K. V. Lew, 'Yield state and stress–strain relationships in a natural plastic clay', *Can. Geotechnol. J*., **20,** 502–516 (1983).
5. Z. Mroz, V. A. Norris and O. C. Zienkiewicz, 'An anisotropic critical state model for soils subject to cyclic loading', *Geotechnique*, **31,** 451–469 (1981).
6. C. S. Desai, S. Somasundaram and G. Frantziskonis, 'A hierarchical approach for constitutive modeling of geologic materials', *Int. J. Numer. Anal. Meth. Geomech*., **10,** 225–257 (1986).
7. B. Muhunthan, J. L. Chameau and E. Masad, Fabric effects on the yield behavior of soils, *Soils Found*., *JSGE*, **36**(3) (1996).
8. J. E. Hilliard, in R. T. De Hoff and F. N. Rhines (eds.) *Measurement of Volume in Volume, Quantitative Microscopy*, McGraw-Hill, New York (1968).
9. B. Muhunthan and J. L. Chameau, 'Void fabric tensor and ultimate state surface of soils', *J. Geotechnol. Engng. Div*., ASCE, **123**(2) (1996).
10. K. Kanatani, 'Stereological determination of structural anisotropy', *Int. J. Engng. Sci*., **22,** 531–546 (1984).
11. Y. F. Dafalias, 'An Anisotropic Critical State Clay Plasticity Model', *Mech. Res. Commun*., **13,** 341–347 (1986).
12. N. Miura, H. Murata and N. Yasufuku, 'Strength characteristics of sand in a particle crushing region', *Soils Found*., *JSSMFE* **24**(1), 77–89 (1984).
13. K. H. Roscoe, A. N. Schofield and A. Thurairajah, 'Yielding of clays in states wetter than critical', *Geotechnique*, **13,** 211–240 (1963).
14. J. B. Burland, Discussion, *Geotechnique*, **15,** 211–214 (1965).
15. K. H. Roscoe and J. B. Burland, On the generalized stress–strain behavior of wet clays, in *Engineering Plasticity*, Cambridge University Press, Cambridge, 1968, pp. 535–609.
16. D. M. Wood, *Soil Behavior and Critical State Soil Mechanics*, Cambridge University Press, Cambridge, 1990.
17. J. H. Atkinson, D. Richardson and P. J. Robinson, Compression and extension of K_0 normally consolidated kaolin clay., *J. Geotechnol. Engng. Div., ASCE*, **113,** 1468–1482 (1987).
18. A. Gens, 'Stress–strain and strength characteristics of a low plasticity clay', *Ph.D. Thesis*, University of London, 1982.
19. J. Graham and G.T. Houlsby, 'Anisotropic elasticity of natural clay', *Geotechnique*, **33,** 165–180 (1983).
20. R. J. Mitchell, 'On the yielding and mechanical strength of Leda clay', *Can. Geotechnol. J*., **7,** 297–312 (1970).

